Pincer-like Amido Complexes of Platinum, Palladium, and Nickel

Jonas C. Peters,* Seth B. Harkins, Steven D. Brown, and Michael W. Day

Division of Chemistry and Chemical Engineering, Arnold and Mabel Beckman Laboratories of Chemical Synthesis, California Institute of Technology, Pasadena, California 91125

Received March 27, 2001

The ligands bis(8-quinolinyl)amine (BQAH, **1**), (2-pyridin-2-yl-ethyl)-(8-quinolinyl)amine (2-pyridin-2-yl-ethyl-QAH, **2**), *o*-dimethylaminophenyl(8-quinolinyl)amine (*o*-(NMe_2)Ph-QAH, **3**), and 3,5-dimethylphenyl(8-quinolinyl)-amine (3,5-Me_2Ph-QAH, **4**) have been prepared in high yield from aryl halide and amine precursors by palladium-catalyzed coupling reactions. Deprotonation of **1** with ^{n}BuLi in toluene affords the lithium amide complex [Li][BQA] (**5**), whose dimeric solid-state crystal structure is presented. Lithium amide **5** was transmetalated by TlOTf to afford the thallium(I) amido complex [Tl][BQA] (**6**). An X-ray structural study of **6** shows it to be a 1:1 complex of the BQA ligand and Tl. Entry into the group 10 chemistry of the parent ligand **1** was effected by both protolytic and metathetical strategies. Thus, the divalent chloride complexes (BQA)PtCl (**7**), (BQA)PdCl (**8**), and (BQA)-NiCl (**9**) were prepared and fully characterized. An X-ray structural study for each of these three complexes shows them to be well-defined, square-planar complexes in which the auxiliary BQA ligand binds in a planar, η^3-fashion. For comparison, the reactivity of ligands **2**−**4** with (COD)$PtCl_2$ was studied. While reaction with ligand **2** afforded an ill-defined product mixture, ligands **3** and **4** reacted with (COD)$PtCl_2$ to generate the unusual alkyl complexes (*o*-(NMe_2)Ph-QA)Pt(1,2-η^2-6-σ-cycloocta-1,4-dienyl) (**10**) and (3,5-Me_2Ph-QA)Pt(1,2-η^2-6-σ-cycloocta-1,4-dienyl) (**11**), both of which have been structurally characterized.

I. Introduction

The study of late transition elements has gained increasing momentum in recent years because of their potential for catalyzing desirable transformations.[1−4] A key feature of later metals is that they tend to be both more tolerant to functional groups and more robust toward air and moisture than their earlier transition metal counterparts.[5,6] In part because of these desirable properties, industrially important late metal polymerization catalysts are now under intense scrutiny.[7] Furthermore, late metal systems are being studied for their ability to couple the activation and oxidation of light hydrocarbon substrates.[8]

To build new molecular systems relevant to these and related goals, our group is pursuing complexes supported by robust, anionic chelating ligands.[9] This manuscript serves two primary purposes. First, it presents a strategy for the synthesis of amido ligands based upon an *N*-(8-quinolinyl) motif. This strategy enables the generation of a readily prepared family of useful, monoanionic amido ligands. Notably, although hard amido ligands can lead to undesirable reduction and/or degradation of late metal complexes, the use of chelating amido ligands can circumvent such problems.[10] Second, this manuscript examines the preparative and structural chemistries of the parent BQA ligand, **1**,[11] with respect to both its synthetically useful lithium and thallium reagents and, more importantly, its ability to coordinate group 10 metal centers in a well-defined, tridentate fashion. Our desire to explore the divalent group 10 chemistry

* To whom correspondence should be addressed. Fax: (626) 577-4088. Tel: (626) 395-4036. E-mail: jpeters@caltech.edu.

(1) Abel, E. W., Stone, F. G. A., Wilkinson, G., Eds. *Comprehensive Organometallic Chemistry*; Elsevier Science, Ltd.: Tarrytown, NY, 1995; Vols. 8−10.
(2) Hegedus, L. S. *Transition Metals in the Synthesis of Complex Organic Molecules*; University Science Books: Mill Valley, CA, 1994.
(3) Doyle, M. P.; Forbes, D. C. *Chem. Rev.* **1998**, *98*, 911.
(4) Gossage, R. A.; VanDeKuil, L. A.; van Koten, G. *Acc. Chem. Res.* **1998**, *31*, 423.
(5) Grubbs, R. H.; Chang, S. *Tetrahedron* **1998**, *54*, 4413.
(6) Joo, F.; Katho, A. *J. Mol. Catal. A: Chem.* **1997**, *116*, 3.
(7) For recent references pertaining to olefin polymerization using cationic mid and late transition metals, see: (a) Ittel, S. D.; Johnson, L. K.; Brookhart, M. *Chem. Rev.* **2000**, *100*, 1169. (b) Killian, C. M.; Johnson, L. K.; Brookhart, M. *Organometallics* **1997**, *16*, 2005. (c) Younkin, T. R.; Conner, E. F.; Henderson, J. I.; Friedrich, S. K.; Grubbs, R. H.; Bansleben, D. A. *Science* **2000**, *287*, 460. (d) Britovsek, G. J. P.; Bruce, M.; Gibson, V. C.; Kimberley, B. S.; Maddox, P. J.; Mastroianni, S.; McTavish, S. J.; Redshaw, C.; Solan, G. A.; Stromberg, S.; White, A. J. P.; Williams, D. J. *J. Am. Chem. Soc.* **1999**, *121*, 8728.
(8) For relevant papers to alkane activation at cationic mid to late metals, see the following: (a) Stahl, S. S.; Labinger, J. A.; Bercaw, J. E. *Angew. Chem., Int. Ed.* **1998**, *37*, 2181. (b) Arndtsen, B. A.; Bergman, R. G.; Mobley, T. A.; Peterson, T. H. *Acc. Chem. Res.* **1995**, *28*, 154. (c) Holtcamp, M. W.; Henling, L. M.; Day, M. W.; Labinger, J. A.; Bercaw, J. E. *Inorg. Chim. Acta* **1998**, *270*, 467. (d) Shen, C. Y.; Garcia-Zayas, E. A.; Sen, A. *J. Am. Chem. Soc.* **2000**, *122*, 4029. (e) Sen, A. *Acc. Chem. Res.* **1998**, *31*, 550. (f) Tellers, D. M.; Bergman, R. G. *J. Am. Chem. Soc.* **2000**, *122*, 954. (g) Periana, R. A.; Taube, D. J.; Gamble, S.; Taube, H.; Satoh, T.; Fujii, H. *Science* **1998**, *280*, 560.
(9) (a) Qian, B. X.; Henling, L. M.; Peters, J. C. *Organometallics* **2000**, *19*, 2805. (b) Thomas, J. C.; Peters, J. C. *J. Am. Chem. Soc.* **2001**, *123*, 5100. (c) Shapiro, I. R.; Jenkins, D. M.; Thomas, J. C.; Day, M. W.; Peters, J. C. *Chem. Commun.*, in press.
(10) For some relevant lead references, see: (a) Fryzuk, M. D.; Macneil, P. A.; Rettig, S. J.; Secco, A. S.; Trotter, J. *Organometallics* **1982**, *1*, 918. (b) Fryzuk, M. D.; Leznoff, D. B.; Thompson, R. C.; Rettig, S. J. *J. Am. Chem. Soc.* **1998**, *120*, 10126. (c) Deacon, G. B.; Gatehouse, B. M.; Grayson, I. L.; Nesbit, M. C. *Polyhedron* **1984**, *3*, 753. (d) Buxton, D. P.; Deacon, G. B.; Gatehouse, B. M.; Grayson, I. L.; Wright, P. J. *Acta Crystallogr., Sect. C* **1985**, *41*, 1049. (e) Dori, Z.; Eisenberg, R.; Steifel, E. I.; Gray, H. B. *J. Am. Chem. Soc.* **1970**, *92*, 1506. (f) Kawamoto, T.; Nagasawa, I.; Kuma, H.; Kushi, Y. *Inorg. Chim. Acta* **1997**, *265*, 163. (g) Endres, H.; Keller, J.; Poveda, A. *Z. Naturforsch., B* **1977**, *32*, 131. (h) Sacco, A.; Vasapollo, G.; Nobile, C. F.; Piergiovanni, A.; Pellinghelli, M. A.; Lanfranchi, M. *J. Organomet. Chem.* **1988**, *356*, 397.
(11) (a) Jenson, K. A.; Nielson, P. H. *Acta Chem. Scand.* **1964**, *18*, 1. (b) Puzas, J. P.; Nakon, R.; Pertersen, J. L. *Inorg. Chem.* **1986**, *25*, 3837.

10.1021/ic010336p CCC: $20.00
Published on Web 08/24/2001

of **1** is motivated, in part, by the following rationale. Square-planar, monoalkyl complexes of ligand **1** should adopt a coordination geometry in which the alkyl group is forced to occupy a coordination site trans to the amido nitrogen donor group. Typically, divalent group 9 and 10 complexes containing two strongly trans-effecting ligands adopt coordination geometries that place these two ligands cis to one another.[12] The BQA ligand discriminates against such a cis preference, and our hope is that resulting complexes will prove reactive at the site trans to the amido nitrogen donor. In this regard, BQA-type ligands are conceptually related to the popular family of anionic "pincer" ligands, a class of ligands that now affords a rich reaction chemistry among metals from groups 8, 9, and 10.[13]

II. Experimental Section

All manipulations were carried out using standard Schlenk or glovebox techniques under a dinitrogen atmosphere. Unless otherwise noted, solvents were deoxygenated and dried by thorough sparging with N_2 gas followed by passage through an activated alumina column. Nonhalogenated solvents were typically tested with a standard purple solution of sodium benzophenone ketyl in tetrahydrofuran to confirm effective oxygen and moisture removal. The reagent 8-bromoquinoline was synthesized following a literature procedure.[14] The preparations of 2-bromo-*N*,*N*-dimethylaniline,[15] (COD)$PdCl_2$,[16] (COD)PdMeCl,[17] (DME)$NiCl_2$,[18] (COD)$PtCl_2$,[19] and (COD)PtMeCl[16] were carried out following literature procedures. Other reagents were purchased from commercial vendors and used without further purification. Elemental analyses were performed by Desert Analytics, Tucson, Az. A Varian Mercury-300 NMR spectrometer or a Varian Inova-500 NMR spectrometer was used to record ^{1}H and ^{13}C NMR spectra unless otherwise stated. ^{1}H and ^{13}C NMR chemical shifts were referenced to residual solvent. MS data for samples were obtained by injection of an acetonitrile solution into a Hewlett-Packard 1100MSD mass spectrometer (ES^+) or an Agilent 5973 mass selective detector (EI). Deuterated chloroform and benzene were degassed and dried over activated 3 Å molecular sieves prior to use.

II.A. Synthesis of BQAH, 1. A 200 mL reaction vessel equipped with a Teflon stopcock and stir bar was charged with $Pd_2(dba)_3$ (0.176 g, 0.192 mmol), *rac*-2,2′-bis(diphenylphosphino)-1,1′-binaphthyl (*rac*-BINAP) (0.239 g, 0.384 mmol), and toluene (30 mL) under a dinitrogen atmosphere. The resulting solution was allowed to stir for 5 min, after which time 8-bromoquinoline (2.00 g, 9.61 mmol), 8-aminoquinoline (1.39 g, 9.64 mmol), and additional toluene (70 mL) were added. The subsequent addition of NaO^{t}Bu (1.11 g, 11.5 mmol) resulted in a red solution that was stirred vigorously for 3 days at 110 °C. The solution was then allowed to cool and filtered through a silica plug that was then extracted with dichloromethane to ensure complete removal of the desired product. Concentration of the collected extracts and removal of solvent yielded a crude red solid (2.37 g, 91%). Purification by flash chromatography on silica gel (4:1 toluene/ethyl acetate) yielded orange, solid bis(8-quinolinyl)amine (1.95 g, 75%) as a spectroscopically pure and synthetically useful compound. Characterization data for **1** compared favorably with that previously reported. ^{1}H NMR ($CDCl_3$, 300 MHz, 25 °C): δ 10.65 (s, 1H), 8.97 (dd, J = 1.7, 2.2 Hz, 2H), 8.16 (dd, J = 1.7, 8.3 Hz, 2H), 7.92 (d, J = 6.5 Hz, 2H), 7.58−7.42 (m, 4H), 7.34 (d, J = 7 Hz, 2H). ^{13}C NMR ($CDCl_3$, 75 MHz, 25 °C): δ 148.1, 140.1, 138.8, 136.2, 129.1, 127.2, 121.7, 117.9, 110.1. LR-MS (electrospray): calcd for $C_{17}H_{17}N_3$ $(M)^+$ m/z 271, found $(M + H)^+$ m/z 272.

II.B. Synthesis of 2-Pyridin-2-yl-ethyl-QAH, 2. A 200 mL reaction vessel with a stir bar was charged with $Pd_2(dba)_3$ (0.170 g, 0.186 mmol), *rac*-2,2′-bis(diphenylphosphino)-1,1′-binaphthyl (*rac*-BINAP) (0.232 g, 0.372 mmol), and toluene (20 mL) under a dinitrogen atmosphere. The resulting solution was allowed to stir for 5 min, after which time 8-bromoquinoline (1.549 g, 7.45 mmol), 2-(2-aminoethyl)pyridine (1.000 g, 8.19 mmol), and additional toluene (20 mL) were added. The subsequent addition of NaO^{t}Bu (1.002 g, 10.43 mmol) caused the reaction slurry to turn red, and the contents were stirred vigorously for 18 h at 90 °C. The final purple solution was cooled to ambient temperature, and the solvent was removed in vacuo affording a viscous violet liquid. Purification by flash chromatography on silica gel (1:1 toluene/ethyl acetate) yielded a red oil that was extracted with diethyl ether, filtered, and dried under vacuum for 24 h to yield the desired product (1.584 g, 85%). ^{1}H NMR ($CDCl_3$, 500 MHz, 25 °C): δ 8.60 (dd, J = 4.2, 1.5 Hz, 1H), 8.51 (d, J = 3.9 Hz, 1H), 7.94 (dd, J = 8.1, 2.0 Hz, 1H), 7.49 (m, 1H), 7.30 (m, 1H), 7.25 (m, 1H), 7.0−7.12 (m, 2H), 6.95 (dd, J = 8.1, 1.5 Hz, 1H), 6.66 (d, J = 6.9 Hz, 1H), 6.31 (br s, N*H*), 3.66 (m, 2H), 3.15 (t, J = 7 Hz, 2H). ^{13}C NMR ($CDCl_3$, 75 MHz, 25 °C): δ 159.8, 149.7, 147.0, 144.8, 138.4, 136.6, 136.1, 128.9, 128.0, 123.6, 121.6, 121.5, 114.0, 104.9, 43.4, 37.9. GC−MS (EI): calcd for $C_{16}H_{15}N_3$ $(M)^+$ m/z 249, found $(M)^+$ m/z 249.

II.C. Synthesis of *o*-(NMe$_2$)Ph-QAH, 3. A 200 mL reaction vessel equipped with a Teflon stopcock and stir bar was charged with $Pd_2(dba)_3$ (0.915 g, 0.999 mmol), 1,1′-bis(diphenylphosphino)ferrocene (DPPF) (1.11 g, 2.00 mmol), and toluene (100 mL) under a dinitrogen atmosphere. The resulting solution was allowed to stir for 5 min, after which time 8-aminoquinoline (3.60 g, 0.0250 mol), *N*,*N*-dimethyl-*o*-bromoaniline (5.00 g, 0.025 mol), and NaO^{t}Bu (2.88 g, 0.030 mol) were added. This solution was stirred vigorously for 3 days at 110 °C after which time it was cooled to room temperature (rt) and filtered through a silica plug. Ethyl acetate was used to elute the plug to ensure complete removal of the desired product. Removal of volatiles in vacuo yielded a crude red liquid. The remaining starting materials were removed via vacuum distillation, and the resulting liquid was filtered once more through a silica gel plug. The orange residue obtained after drying in vacuo (3.56 g, 54%) solidified upon standing at rt for 5 days. ^{1}H NMR ($CDCl_3$, 300 MHz, 25 °C): δ 8.85 (dd, J = 1.8, 4.2 Hz, 1 H), 8.71 (s, 1H), 8.13 (dd, J = 1.5, 8.1 Hz, 1 H), 7.67 (dd, J = 1.8, 8.1 Hz, 1H), 7.60 (dd, J = 1.2, 7.8 Hz, 1H), 7.45 (dd, J = 1.5, 6.0 Hz, 1H), 7.43 (m, 1H), 7.24−6.97 (m, 5H), 2.75 (s, 6H). ^{13}C NMR ($CDCl_3$, 75 MHz, 25 °C): δ 147.6, 145.1, 140.0, 139.3, 136.1, 136.0, 129.1, 127.4, 123.2, 121.6, 119.4, 117.8, 116.4, 107.8, 44.1. LR-MS (electrospray): calcd for $C_{17}H_{17}N_3$ $(M)^+$ m/z 263, found $(M + H)^+$ m/z 264.

II.D. Synthesis of 3,5-Me$_2$Ph-QAH, 4. A 200 mL reaction vessel equipped with a Teflon stopcock and stir bar was charged with $Pd_2(dba)_3$ (0.222 g, 0.242 mmol), 1,1′-bis(diphenylphosphino)ferrocene (DPPF) (0.268 g, 0.483 mmol), and 20 mL of toluene under a dinitrogen atmosphere. The resulting solution was allowed to stir for 5 min, after which time 8-aminoquinoline (0.873 g, 6.05 mmol), 3,5-dimethylbromobenzene (1.12 g, 6.05 mmol), and NaO^{t}Bu (1.16 g, 12.1 mmol) were added. The solution was allowed to stir at 110 °C for 24 h, after which time it was allowed to cool and filtered over silica gel. Toluene was then removed in vacuo, and flash chromatography on silica gel (15:1 toluene/ethyl acetate) yielded spectroscopically pure **4** as an orange liquid (1.28 g, 85%). ^{1}H NMR ($CDCl_3$, 300 MHz, 25 °C): δ 8.79 (dd, J = 1.5, 4.2 Hz, 1H), 8.21 (s, 1H), 8.12 (dd, J = 1.8, 8.4 Hz, 1H), 7.52−7.20 (m, 4H), 7.05 (s, 2H), 6.72 (s, 1H), 2.40 (s, 6H). ^{13}C NMR ($CDCl_3$, 75 MHz, 25 °C): δ 147.3, 141.8, 140.5, 139.1, 138.3, 136.3, 129.0, 128.5, 124.1, 121.7, 118.0, 116.3, 108.0, 21.8. LR-MS (electrospray): calcd for $C_{17}H_{16}N_2$ (M^+) m/z 248, found $(M + H)^+$ m/z 249.

(12) (a) Vila, J. M.; Pereira, M. T.; Ortigueira, J. M.; Lata, D.; Lopez Torres, M.; Fernandez, J. J.; Fernandez, A.; Adams, H. *J. Organomet. Chem.* **1998**, *566*, 93. (b) Crespo, M.; Solans, X.; Font-Bardia, M. *Polyhedron* **1998**, *17*, 3927. (c) Gandelman, M.; Vigalok, A.; Shimon, L. J. W.; Milstein, D. *Organometallics* **1997**, *16*, 3981.
(13) (a) Liu, F. C.; Pak, E. B.; Singh, B.; Jensen, C. M.; Goldman, A. S. *J. Am. Chem. Soc.* **1999**, *121*, 4086. (b) Sundermann, A.; Uzan, O.; Milstein, D.; Martin, J. M. L. *J. Am. Chem. Soc.* **2000**, *122*, 7095. (c) Dani, P.; Karlen, T.; Gossage, R. A.; Gladiali, S.; van Koten, C. *Angew. Chem., Int. Ed.* **2000**, *39*, 743.
(14) Butler, J. L.; Gordon, M. *J. Heterocycl. Chem.* **1975**, *12*, 1015.
(15) Kelly, D. P.; Bateman, S. A.; Hook, R. J.; Martin, R. F.; Reum, M.; Rose, M.; Whittaker, A. R. D. *Aust. J. Chem.* **1994**, *47*, 1751.
(16) Chatt, L.; Vallarino, L. M. *J. Chem. Soc.* **1957**, 3413.
(17) lke, R. E.; Ernsting, J. M.; Spek, A. L.; Elsevier, C. J.; van Leewen, P. W. N. M.; Vrieze, K. *Inorg. Chem.* **1993**, *32*, 5769.
(18) Ward, L. G. L. *Inorg. Synth.* **1971**, *13*, 154.
(19) Clark, H. C.; Manzer, L. E. *J. Organomet. Chem.* **1973,** *59*, 411.

II.E. Synthesis of [Li][BQA], 5. A solution of 1.6 M *n*-butyllithium in hexanes (4.82 mL, 7.71 mmol) diluted with toluene (20 mL) was added dropwise over 30 min to a stirring solution of BQAH (2.089 g, 7.71 mmol) in toluene (250 mL) at −78 °C. The reaction mixture was then allowed to warm slowly to ambient temperature. After the reaction mixture was stirred for an additional 24 h, the solvent was removed in vacuo, affording a bright orange solid. The product was lyophilized from 50 mL of benzene, washed with petroleum ether (3 × 30 mL), and dried in vacuo affording spectroscopically pure **5** (1.880 g, 88%). ^{1}H NMR ($CDCl_3$, 300 MHz, 25 °C): δ 7.84 (d, J = 7.7 Hz, 2H), 7.70 (d, J = 8.2 Hz, 2H), 7.54 (d, J = 4.5 Hz, 2H), 7.31 (m, 2H), 6.81 (d, J = 7.7 Hz, 2H), 6.69 (m, 2H). ^{13}C NMR ($CDCl_3$, 126 MHz, 25 °C): δ 156.0, 145.3, 145.2, 136.3, 130.3, 128.3, 120.0, 113.6, 112.4. Anal. Calcd for $C_{18}H_{12}N_3Li$: C, 77.98; H, 4.36; N, 15.16. Found: C, 77.92; H, 4.41; N, 14.39.

II.F. Synthesis of [Tl][BQA], 6. [Li][BQA] (500 mg, 1.803 mmol) and thallium triflate (637 mg, 1.803 mmol) were dissolved separately in THF (25 mL) and cooled to −30 °C. The thallium triflate was then added to the [Li][BQA] quickly, and the solution was stirred for 48 h at ambient temperature. THF was removed in vacuo, and the resulting red residue was extracted with benzene, filtered through Celite, and dried by benzene lyophilization to afford a red powder. The crude product was washed with petroleum ether (5 × 30 mL) and dried to afford **6** (454 mg, 53%). The product contained trace impurities of LiOTf, the complete removal of which has thus far proved problematic. ^{1}H and ^{13}C NMR, in addition to an X-ray diffraction study of a single crystal obtained by vapor diffusion of petroleum ether into a benzene solution, all support the assignment of the thallium complex **6**. ^{1}H NMR (C_6D_6, 300 MHz, 25 °C): δ 8.09 (br s, 2H), 7.72 (d, J = 7.5 Hz, 2H), 7.51 (d, J = 8.4 Hz, 2H), 7.29 (m, 2H), 6.81 (d, J = 7.8 Hz, 2H), 6.70 (br s, 2H). ^{13}C NMR (C_6D_6, 75 MHz, 25 °C): δ 154.9, 145.7, 144.6, 137.8, 132.5, 127.9, 121.0, 114.9, 114.1.

II.G. Synthesis of (BQA)PtCl, 7. A benzene solution (20 mL) of [Li][BQA] (370.5 mg, 1.336 mmol) was quickly added to a flask containing (COD)$PtCl_2$ (500 mg, 1.336 mmol) dissolved in benzene (30 mL) that had been chilled to −35 °C. The stirring reaction solution was allowed to warm slowly and was subsequently heated at 65 °C for an additional 20 h. The resulting intense purple solution was filtered through Celite, followed by additional washings with dichloromethane (3 × 10 mL). Solvent was removed from the filtrate in vacuo. The resulting purple solid was washed with petroleum ether (3 × 30 mL) and dried, affording a purple powder (454 mg, 68%). This powder was easily recrystallized in a hexane/chloroform diffusion chamber. ^{1}H NMR ($CDCl_3$, 300 MHz, 25 °C): δ 9.14 (d, J = 5.0 Hz, 2H, $^3J_{PtH}$ = 37 Hz), 8.23 (d, J = 8.3 Hz, 2H), 7.62 (d, J = 8.0 Hz, 2H), 7.43 (m, 2H), 7.37 (m, 2H), 7.02 (d, J = 8.4 Hz, 2H). ^{13}C NMR ($CDCl_3$, 75 MHz, 25 °C): δ 148.8, 148.7, 148.4, 138.9, 131.4, 129.4, 121.2, 115.7, 113.6. LR-MS (electrospray): calcd for $C_{18}H_{12}ClN_3Pt$ $(M)^+$ m/z 500, found $(M + H)^+$ m/z 501. Anal. Calcd for $C_{18}H_{12}ClN_3Pt$: C, 43.17; H, 2.42; N, 8.39. Found: C, 42.81; H, 2.47; N, 8.03.

II.H. Alternative Synthesis of 7. To a reaction vessel containing **1** (1.00 g, 3.6 mmol) and (COD)$PtCl_2$ (1.346 g, 3.6 mmol) dissolved in THF (30 mL), triethylamine (651 μL, 4.68 mmol) was added in one portion. The vessel was sealed and stirred at 95 °C for 48 h. The resulting red solution was cooled and dried in vacuo, extracted with CH_2Cl_2 (50 mL), and filtered through Celite on a sintered-glass frit. The solvent was again removed under reduced pressure, and the precipitate was washed with methanol (3 × 30 mL) and petroleum ether (2 × 10 mL) and then dried in vacuo to give the desired product (1.176 g, 65%). Spectral data were consistent with those reported above.

II.I. Synthesis of (BQA)PdCl, 8. To a reaction flask containing (COD)$PdCl_2$ (1.05 g, 3.6 mmol) dissolved in THF (75 mL) was added a THF solution of **1** (1.00 g, 3.6 mmol) and triethylamine (651 μL, 4.68 mmol). The vessel was sealed and heated at 95 °C for 48 h. After the reaction was cooled, the reaction solution volatiles were removed in vacuo, affording a red residue. This crude product was dissolved in CH_2Cl_2 (50 mL), filtered through Celite on a sintered-glass frit, and washed with dilute brine solution (3 × 20 mL). The volume was reduced in vacuo, and the product was precipitated from solution with hexanes. The resulting red microcrystalline solid was washed with petroleum ether (3 × 15 mL) and dried to afford spectroscopically pure product **8** (915 mg, 62%). An analytically pure sample was obtained from a hexanes/chloroform diffusion chamber. ^{1}H NMR ($CDCl_3$, 300 MHz, 25 °C): δ 8.95 (d, J = 5 Hz, 2H), 8.20 (d, J = 8.2 Hz, 2H), 7.65 (d, J = 8.2 Hz, 2H), 7.46 (m, 2H), 7.37 (m, 2H), 7.07 (d, J = 8.2 Hz, 2H). ^{13}C NMR ($CDCl_3$, 75 MHz, 25 °C): δ 149.5, 148.9, 148.3, 138.8, 131.2, 129.5, 121.3, 115.1, 112.6. LR-MS (electrospray): calcd for $C_{18}H_{12}ClN_3Pd$ $(M)^+$ m/z 411, found $(M - Cl)^+$ m/z 376. Anal. Calcd for $C_{18}H_{12}N_3PdCl$: C, 52.45; H, 2.93; N, 10.19. Found: C, 52.17; H, 2.92; N, 9.80.

II.J. Alternative Synthesis of 8. A solution of **5** (0.100 g, 0.361 mmol) in dichloromethane (5 mL) was added dropwise to a stirring solution of (COD)$PdCl_2$ (0.103 g, 0.361 mmol) in dichloromethane (10 mL). The solution became red-brown immediately upon addition. The reaction solution was stirred at 62 °C for 24 h, after which time it was cooled and dried in vacuo. The red solid was washed successively with ethanol (3 × 10 mL), diethyl ether (2 × 10 mL), and pentane (2 × 10 mL) and then dried thoroughly under reduced pressure to yield a red solid (114 mg, 77%). Spectral data were analogous with those reported above.

II.K. Synthesis of (BQA)NiCl, 9. A 200 mL reaction bomb was charged with **5** (200 mg, 0.722 mmol) dissolved in THF (50 mL). A slurry of (DME)$NiCl_2$ in THF (10 mL) was added to the stirring purple solution. The solution began to turn red immediately upon addition. The vessel was sealed with a Teflon stopcock and heated at 62 °C for 20 h. The reaction solution was allowed to cool, and the solvent was removed in vacuo. The resulting red solid was washed with Et_2O (50 mL), and LiCl was removed by extraction with EtOH (4 × 30 mL) followed by Et_2O (2 × 10 mL). The product was dried for 24 h under reduced pressure to yield a microcrystalline red solid (220 mg, 84%). Complex **9** may be recrystallized from a hexanes/chloroform diffusion chamber. ^{1}H NMR ($CDCl_3$, 300 MHz, 25 °C): δ 8.66 (d, J = 5 Hz, 2H), 8.13 (d, J = 8 Hz, 2H), 7.49 (d, J = 8 Hz, 2H), 7.40 (m, 2H), 7.27 (m, 2H), 6.95 (d, J = 8 Hz, 2H). ^{13}C NMR ($CDCl_3$, 75 MHz, 25 °C): δ 150.6, 148.0, 147.8, 138.7, 129.8, 129.5, 121.3, 114.0, 111.7. LR-MS (electrospray): calcd for $C_{18}H_{12}ClN_3Ni$ $(M)^+$ m/z 363, found $(M - Cl)^+$ m/z 328. Anal. Calcd for $C_{18}H_{12}N_3ClNi$: C, 59.32; H, 3.32; N, 11.53. Found: C, 59.19; H, 3.31; N, 11.33.

II.L. Alternative Synthesis of 9. Ligand **1** (0.123 g, 0.455 mmol) and (DME)$NiCl_2$ (0.100 g, 0.455 mmol) were dissolved in THF (10 mL) at ambient temperature. An aliquot of triethylamine (190 μL, 1.365 mmol) was added in one portion. Within several minutes, the reaction solution became red. Stirring was continued at 62 °C for 24 h. The resulting red solution was cooled and dried in vacuo. The solid product was then washed successively with ethanol (3 × 10 mL), diethyl ether (2 × 10 mL), and pentane (2 × 10 mL) and dried under reduced pressure for 24 h to yield **9** (147 mg, 89%). Spectral data were consistent with those reported above.

II.M. Synthesis of (*o*-(NMe_2)Ph-QA)Pt(1,2-η^2-6-σ-cycloocta-1,4-dienyl), 10. A 2 mL CH_2Cl_2 solution of (0.0706 g, 0.268 mmol) and NEt_3 (0.0814 g, 0.804 mmol) was added dropwise to a stirring solution of (COD)$PtCl_2$ (0.100 g, 0.268 mmol) in 3 mL of CH_2Cl_2. The reaction gradually turned red in color and was allowed to stir for 24 h at rt, after which time the volatiles were removed in vacuo. The resulting crude red solid was then dissolved in 5 mL of benzene, filtered, and lyophilized. Trituration with petroleum ether (3 × 3 mL) followed by drying in vacuo yielded the analytically pure product (0.148 g, 98%) as a mixture of two spectroscopically observable isomers in a 3:1 ratio (vide infra). X-ray quality crystals were grown by vapor diffusion of petroleum ether into a benzene solution of **10**. Because of overlapping resonances resulting from the two isomers, it was not possible to reliably integrate the ^{1}H NMR spectrum. The observed resonances for the ^{1}H and ^{13}C NMR are reported. ^{1}H NMR ($CDCl_3$, 300 MHz, 25 °C): δ 8.20 (dd, J = 1.0, 8.0 Hz), 8.04 (dd, J = 1.0, 4.8 Hz, $^3J_{PtH}$ = 17 Hz), 6.93−7.45 (m), 6.76 (m), 6.31 (m), 5.53 (m), 5.34 (m), 4.93 (m, $^2J_{PtH}$ = 72 Hz), 4.62 (m, $^2J_{PtH}$ = 72 Hz), 3.57 (m), 3.00−3.2 (m), 2.77 (m, NMe_2, major isomer), 2.72 (m, NMe_2, minor isomer), 1.20−2.0 (m). ^{13}C NMR ($CDCl_3$, 75 MHz, 25 °C): δ 156.9, 149.3, 141.9, 142.2, 141.7, 138.0, 135.8, 135.4, 133.9, 130.5, 130.4, 130.3, 130.2, 129.4, 129.0, 128.3, 126.8, 125.2, 121.5, 121.2, 121.0, 120.9, 118.2, 117.4, 110.7, 110.6, 109.9, 76.7, 71.0, 53.3, 46.4, 43.7, 42.8, 40.9, 40.4, 40.2, 36.4,

33.7, 31.7, 28.9, 28.7, 28.3, 27.0, 25.6, 25.0, 24.9, 9.29, 8.50. LR-MS (electrospray): calcd for $C_{25}H_{27}N_3Pt$ $(M)^+$ *m*/*z* 564, found $(M + H)^+$ *m*/*z* 565. Anal. Calcd for $C_{25}H_{27}N_3Pt$: C, 53.18; H, 4.82; N, 7.44. Found: C, 53.45; H, 4.75; N, 7.19.

II.N. Synthesis of (3,5-Me$_2$Ph-QA)Pt(1,2-η^2-6-σ-cycloocta-1,4-dienyl), 11. A 2 mL CH_2Cl_2 solution of **4** (0.0666 g, 0.268 mmol) and NEt_3 (0.0814 g, 0.804 mmol) was added dropwise to a stirring solution of $(COD)PtCl_2$ (0.100 g, 0.268 mmol) in 3 mL of CH_2Cl_2. The reaction gradually turned red in color and was allowed to stir for 24 h at rt, after which time the volatiles were removed in vacuo. The resulting crude red solid was then dissolved in 5 mL of benzene, filtered, and lyophilized. Trituration with petroleum ether (3 × 3 mL) followed by drying in vacuo yielded a spectroscopically pure product (0.140 g, 95%). X-ray quality crystals were grown from vapor diffusion of petroleum ether into benzene. ^{1}H NMR ($CDCl_3$, 300 MHz, 25 °C): δ 8.20 (dd, J = 1.0, 8.4 Hz, 1H), 8.05 (dd, J = 1.0, 4.5 Hz, 1H, $^3J_{PtH}$ = 17 Hz), 7.41 (m, 1H), 7.25 (m, 1H), 6.87 (s, 2H), 6.83 (s, 1H), 6.77 (d, J = 8.1 Hz, 1H), 6.60 (d, J = 8.1 Hz, 1H), 5.54 (m, 1H), 5.36 (m, 1H), 4.97 (m, 1H, $^2J_{PtH}$ = 72 Hz), 4.65 (m, 1H, $^2J_{PtH}$ = 72 Hz), 3.16 (m, 1H), 2.80 (m, 1H), 2.35 (s, 6H), 2.00−1.32 (m, 5H). ^{13}C NMR ($CDCl_3$, 75 MHz, 25 °C): δ 159.1, 150.4, 142.1, 138.5, 138.0, 135.5, 131.2, 130.4, 129.0, 128.5, 125.9, 125.7, 121.2, 111.1, 109.5, 77.2, 70.7, 41.0, 31.5, 28.8, 24.9, 21.8. LR-MS (electrospray): calcd for $C_{25}H_{26}N_2Pt$ $(M)^+$ *m*/*z* 549, found $(M + H)^+$ *m*/*z* 550. Anal. Calcd for $C_{25}H_{26}N_2Pt$: C, 54.64; H, 4.77; N, 5.10. Found: C, 54.61; H, 5.01; N, 4.99.

II.O. X-ray Crystal Structure Analysis of [Li][BQA], 5. X-ray quality crystals were obtained from a benzene/petroleum ether diffusion chamber at 25 °C. A red crystalline blade was mounted on a glass fiber with Paratone-N oil (an Exxon product). The structure was solved by direct methods in conjunction with standard difference Fourier techniques. The largest peak and hole in the difference map were 0.351 and −0.195 e Å^{-3}, respectively. Maximum and minimum transmissions were equal to 0.9971 and 0.9684, respectively. Crystal data for $C_{36}H_{24}Li_2N_6$: monoclinic space group $P2_1/c$ (No. 14), a = 22.490(3) Å, b = 8.6035(10) Å, c = 14.4810(17) Å, β = 97.875(2)°, V = 2775.5(6) Å^3, Z = 4, D_{calcd} = 1.327 g cm^{-3}, abs coefficient = 0.079 mm^{-1}, λ(Mo Kα) = 0.710 73 Å, T = 98(2) K, Bruker SMART 1000 CCD, crystal size = 0.41 × 0.3 × 0.04 mm^3, θ_{max} = 28.36°, R1 = 0.0525, wR2 = 0.0835, for $I > 2\sigma(I)$ R1 = 0.1141, wR2 = 0.0877, number of reflections collected = 39470 ($-29 \le h \le 29$, $-11 \le k \le 11$, $-19 \le l \le 18$), number of independent reflections = 6569, number of parameters = 493.

II.P. X-ray Crystal Structure Analysis of [Tl][BQA], 6. X-ray quality crystals were obtained from a benzene/petroleum ether diffusion chamber at 25 °C. A red crystalline blade was mounted on a glass fiber with Paratone-N oil. The structure was solved by direct methods in conjunction with standard difference Fourier techniques. The largest peak and hole in the difference map were 1.738 and −1.191 e Å^{-3}, respectively. SADABS data correction was applied on the basis of pseudo-ψ scans with maximum and minimum transmissions equal to 0.7535 and 0.7213, respectively. Crystal data for $C_{18}H_{12}N_3Tl$: orthorhombic space group $Pna2_1$ (No. 33), a = 6.9767(11) Å, b = 23.289(4) Å, c = 8.7724(13) Å, V = 1425.3(4) Å^3, Z = 4, D_{calcd} = 2.212 g cm^{-3}, abs coefficient = 11.330 mm^{-1}, λ(Mo Kα) = 0.710 73 Å, T = 98(2) K, Bruker SMART 1000 CCD, crystal size = 0.89 × 0.23 × 0.16 mm^3, θ_{max} = 28.39°, R1 = 0.0245, wR2 = 0.0397, for $I > 2\sigma(I)$ R1 = 0.0336, wR2 = 0.0405, number of reflections collected = 22995 ($-9 \le h \le 8$, $-29 \le k \le 30$, $-11 \le l \le 11$), number of independent reflections = 3324, number of parameters = 199.

II.Q. X-ray Crystal Structure Analysis of (BQA)PtCl, 7. X-ray quality crystals were obtained from a chloroform/petroleum ether diffusion chamber at 25 °C. A dark red crystalline column was mounted on a glass fiber with Paratone-N oil. The structure was solved by direct methods in conjunction with standard difference Fourier techniques. The largest peak and hole in the difference map were 1.015 and −0.976 e Å^{-3}, respectively. SADABS data correction was applied on the basis of pseudo-ψ scans with maximum and minimum transmissions equal to 1.0000 and 0.5322, respectively. Crystal data for $C_{18}H_{12}ClN_3Pt$: monoclinic space group $P2_1/n$ (No. 14), a = 9.1532(12) Å, b = 11.5481(15) Å, c = 15.1060(19) Å, β = 106.997(2)°, V = 1527.0(3) Å^3, Z = 4, D_{calcd} = 2.179 g cm^{-3}, abs coefficient = 9.365 mm^{-1}, λ(Mo Kα) = 0.71073 Å, T = 98(2) K, Bruker SMART 1000 CCD, crystal size = 0.28 × 0.22 × 0.22 mm^3, θ_{max} = 28.31°, R1 = 0.0245, wR2 = 0.0452, for $I > 2\sigma(I)$ R1 = 0.0331, wR2 = 0.0460, number of reflections collected = 26365 ($-11 \le h \le 12$, $-14 \le k \le 15$, $-19 \le l \le 19$), number of independent reflections = 3635, number of parameters = 256.

II.R. X-ray Crystal Structure Analysis of (BQA)PdCl, 8. X-ray quality crystals were obtained from a chloroform/petroleum ether diffusion chamber at 25 °C. A dark red crystalline column was mounted on a glass fiber with Paratone-N oil. The structure was solved by direct methods in conjunction with standard difference Fourier techniques. The largest peak and hole in the difference map were 0.587 and −0.522 e Å^{-3}, respectively. No data correction was applied. Maximum and minimum transmissions were equal to 0.7428 and 0.6828, respectively. Crystal data for $C_{18}H_{12}ClN_3Pd$: monoclinic space group $P2_1/n$ (No. 14), a = 7.5343(7) Å, b = 14.9983(14) Å, c = 12.8184(12) Å, β = 93.845(2)°, V = 1445.2(2) Å^3, Z = 4, D_{calcd} = 1.894 g cm^{-3}, abs coefficient = 1.470 mm^{-1}, λ(Mo Kα) = 0.71073 Å, T = 98(2) K, Bruker SMART 1000 CCD, crystal size = 0.28 × 0.22 × 0.22 mm^3, θ_{max} = 28.06°, R1 = 0.0267, wR2 = 0.0544, for $I > 2\sigma(I)$ R1 = 0.0318, wR2 = 0.0549, number of reflections collected = 20400 ($-9 \le h \le 9$, $-18 \le k \le 19$, $-16 \le l \le 16$), number of independent reflections = 3343, number of parameters = 256.

II.S. X-ray Crystal Structure Analysis of (BQA)NiCl, 9. X-ray quality crystals were obtained from a chloroform/hexanes diffusion chamber at 25 °C. A dark red crystalline block was mounted on a glass fiber with Paratone-N oil. The structure was solved by direct methods in conjunction with standard difference Fourier techniques. The largest peak and hole in the difference map were 0.309 and −0.377 e Å^{-3}, respectively. Maximum and minimum transmissions were equal to 0.7535 and 0.7213, respectively. Crystal data for $C_{18}H_{12}ClN_3Ni$: monoclinic space group $P2_1/n$ (No. 14), a = 8.9635(7) Å, b = 11.4785(9) Å, c = 14.9909(12) Å, β = 107.3220(10)°, V = 1472.4(2) Å^3, Z = 4, D_{calcd} = 1.644 g cm^{-3}, abs coefficient = 1.500 mm^{-1}, λ(Mo Kα) = 0.71073 Å, T = 98(2) K, Bruker SMART 1000 CCD, crystal size = 0.23 × 0.20 × 0.20 mm^3, θ_{max} = 28.26°, R1 = 0.0317, wR2 = 0.0615, for $I > 2\sigma(I)$ R1 = 0.0426, wR2 = 0.0627, number of reflections collected = 20863 ($-11 \le h \le 11$, $-15 \le k \le 14$, $-19 \le l \le 19$), number of independent reflections = 3452, number of parameters = 256.

II.T. X-ray Crystal Structure Analysis of (*o*-(NMe$_2$)Ph-QAH)-Pt(1,2-η^2-6-σ-cycloocta-1,4-dienyl), 10a. X-ray quality crystals were obtained from a benzene/petroleum ether diffusion chamber at 25 °C. A red crystalline block was mounted on a glass fiber with Paratone-N oil. The structure was solved by direct methods in conjunction with standard difference Fourier techniques. The largest peak and hole in the difference map were 1.488 and −0.577 e Å^{-3}, respectively. Maximum and minimum transmissions were equal to 1.0000 and 0.7282, respectively. Crystal data for $C_{25}H_{27}N_3Pt$: triclinic space group $P\bar{1}$ (No. 2), a = 7.5521(7) Å, b = 10.7997(9) Å, c = 13.4693(12) Å, α = 108.3110(10)°, β = 107.3220(10)°, γ = 94.7070(10)°, V = 1034.23(16) Å^3, Z = 2, D_{calcd} = 1.813 g cm^{-3}, abs coefficient = 6.800 mm^{-1}, λ(Mo Kα) = 0.71073 Å, T = 98(2) K, Bruker SMART 1000 CCD, crystal size = 0.22 × 0.19 × 0.15 mm^3, θ_{max} = 28.31°, R1 = 0.0237, wR2 = 0.0413, for $I > 2\sigma(I)$ R1 = 0.0204, wR2 = 0.0410, number of reflections collected = 15396 ($-9 \le h \le 10$, $-14 \le k \le 14$, $-17 \le l \le 17$), number of independent reflections = 4745, number of parameters = 370.

II.U. X-ray Crystal Structure Analysis of (3,5-Me$_2$Ph-QA)Pt(1,2-η^2-6-σ-cycloocta-1,4-dienyl), 11. X-ray quality crystals were obtained from a benzene/petroleum ether diffusion chamber at 25 °C. A red crystalline block was mounted on a glass fiber with Paratone-N oil. The structure was solved by direct methods in conjunction with standard difference Fourier techniques. The largest peak and hole in the difference map were 1.357 and −0.496 e Å^{-3}, respectively. Maximum and minimum transmissions were equal to 1.0000 and 0.6946, respectively. Crystal data for $C_{25}H_{26}N_2Pt$: orthorhombic space group $P2_12_12_1$, a = 9.2884(7) Å, b = 11.4127(9) Å, c = 19.3116(12) Å, V = 2047.1(3) Å^3, Z = 4, D_{calcd} = 1.783 g cm^{-3}, abs coefficient = 6.867 mm^{-1}, λ(Mo Kα) = 0.71073 Å, T = 98(2) K, Bruker SMART 1000

CCD, crystal size = 0.29 × 0.13 × 0.07 mm^3, θ_{max} = 28.46°, R1 = 0.0210, wR2 = 0.0347, for $I > 2\sigma(I)$ R1 = 0.0192, wR2 = 0.0344, number of reflections collected = 30635 ($-12 \le h \le 12$, $-14 \le k \le 15$, $-25 \le l \le 25$), number of independent reflections = 4878, number of parameters = 335.

III. Results and Discussion

III.A. Preparation of Ligands. A synthetic strategy for the preparation of amines **1**−**4** exploits Pd-coupling methodology for N−C bond formation, a transformation that has recently matured because of the efforts of the respective research groups of Buchwald and Hartwig.[20] A new synthesis of the previously prepared amine **1** provided a good starting point for several reasons. First, in our hands, the literature preparation of **1** afforded unacceptably low yields (typically less than 10%) of the desired product ligand and was simultaneously time-consuming and very tedious.[11] Direct coupling of commercially available 8-aminoquinoline with 8-bromoquinoline promised to be a more elegant preparation of **1** in comparison to the low-yielding Bucherer reaction by which it was originally synthesized. Second, although **1** was first prepared nearly four decades ago, only a single transition metal complex, (BQA)CuCl,[11] has been definitively characterized supported by this potentially versatile auxiliary ligand. We anticipated that **1** and related amines would yield to a rich reaction chemistry among the transition elements and hence set about its improved preparation.

It was found that the reaction between 8-bromoquinoline and 8-aminoquinoline under standard coupling conditions ($Pd_2(dba)_3$, toluene, 110 °C) with NaO^{t}Bu as the base and *rac*-BINAP as the cocatalyst provided reliably high yields of **1**. The product was readily isolated by flash chromatography and analyzed by LR-MS and ^{1}H and ^{13}C NMR spectroscopies. The data for **1** compared favorably with those for **1** obtained by its independent preparation following the literature procedure.[11] Ligand **1** has been prepared on multigram scales in isolated yields typically greater than 80%. A catalyst loading of 2−4% is sufficient: an isolated yield of 94% has been obtained with a 4% catalyst loading. Notably, **1**, while an excellent chelating ligand for palladium (vide infra), does not poison the catalyst system.

Hoping to extend this methodology to three related amines, we attempted the synthesis of 2-pyridin-2-yl-ethyl-QAH (**2**), *o*-(NMe_2)Ph-QAH (**3**), and 3,5-Me_2Ph-QAH (**4**) under the same conditions.[21] The reaction worked well for **2** but proved sluggish for **3** and **4**. A survey of other cocatalysts established DPPF (DPPF = bis(diphenylphosphino)ferrocene) as a viable alternative for the preparation of both **3** and **4** in satisfactory isolated yield after flash chromatography. The syntheses for ligands **1**−**4** are summarized in Scheme 1. These anionic amido ligands are related in that each can provide a metal atom with one amido N-donor group and one or two neutral nitrogen donor groups. Ligand **1**, the chemistry of which is the primary focus of this manuscript, provides two symmetrical quinolinyl donor arms capable of forming two fused five-membered rings upon metalation. This motif has now been structurally established for several square-planar (vide infra) and octahedral complexes of **1**.[22]

Scheme 1

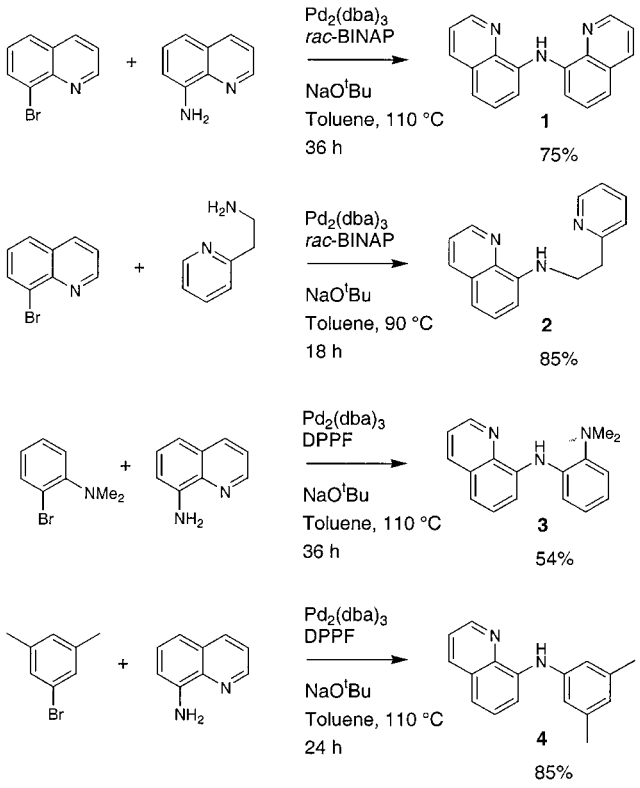

III.B. Preparation and Structural Characterization of the Lithium and Thallium Derivatives, [Li][BQA] (5) and [Tl][BQA] (6). To explore the coordination chemistry of **1**, we first sought a reliable preparative procedure for its lithiation. Of immediate concern to us was that employment of the typical ^{n}BuLi base for deprotonation might result in competitive nucleophilic attack at the relatively electrophilic 2-carbon position of the quinoline ring. Indeed, when a stoichiometric amount of ^{n}BuLi is added slowly to a toluene solution of **1** at ambient temperature, significant side products result from competitive alkylation; these byproducts are difficult to separate from the major product, **5**. Fortunately, slow dropwise addition of a dilute solution of ^{n}BuLi to **1** at −78 °C circumvents kinetically competitive alkylation products, and the intensely orange lithium complex **5** is formed cleanly in the absence of donor solvent (Scheme 2). The amide **5** is unusual in that it is both soluble and stable in halogenated solvents such as chloroform and methylene chloride.

To examine its solid-state structure, crystals suitable for an X-ray diffraction study were obtained by slow diffusion of petroleum ether into a benzene solution. The structure of **5**, shown in Figure 1, shows a dimeric complex in which two lithium cations, LiA and LiB, and two bridging amido nitrogens, N(2A) and N(2B), join to form a parallelepiped that bisects the dimeric molecule. Each of the two donor quinolinyl arms of the amido ligands binds a different lithium cation, imparting a twisted structure to the molecule, the idealized molecular

(20) (a) Wolfe, J. P.; Tomori, H.; Sadighi, J. P.; Yin, J. J.; Buchwald, S. L. *J. Org. Chem.* **2000**, *65*, 1158. (b) Alcazar-Roman, L. M.; Hartwig, J. F.; Rheingold, A. L.; Liable-Sands, L. M.; Guzei, I. A. *J. Am. Chem. Soc.* **2000**, *122*, 4618. (c) Hartwig, J. F. *Acc. Chem. Res.* **1998**, *31*, 852. (d) Hamamm, B. C.; Hartwig, J. F. *J. Am. Chem. Soc.* **1998**, *120*, 12706.

(21) In this manuscript we have adopted the following simplification for naming ligands **1**−**4**: The ligands are all derived from the primary amine 8-quinolinylamine (abbreviated as QAH in this manuscript). The second substituent at nitrogen, affording the secondary amine, is written explicitly in conjunction with QAH. Thus, (*o*-NMe_2Ph-QAH) implies that 8-aminoquinoline is substituted by an aryl group containing a dimethylamino group in the ortho position. When bound to a metal as an anionic amido ligand, the H is dropped from QAH, as in (BQA)PtCl.

(22) Betley, T.; Brown, S. D.; Harkins, S. B.; Qian, B.; Peters, J. C. Unpublished results.

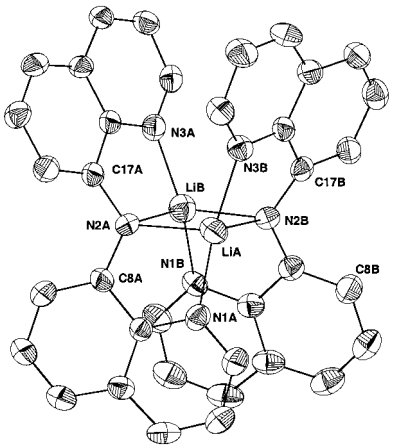

Figure 1. Displacement ellipsoid (50%) representation of [Li][BQA] (**5**). Selected bond distances (Å) and angles (deg) are as follows: LiA−N(1A), 2.024(4); LiA−N(2A), 2.079(4); LiA−N(2B), 2.063(4); LiA−N(3B), 1.990(4); LiA−LiB, 2.395(5); LiB−N(1B), 1.958(4); LiB−N(2B), 2.051(4); LiB−N(2A), 2.018(4); LiB−N(3A), 1.999(4); N(2B)−LiA−N(2A), 107.15(18); N(2A)−LiA−LiB, 53.05(13); N(2B)−LiA−LiB, 54.16(13); N(2B)−LiA−N(2A), 107.15(18); N(1A)−LiA−N(2A), 82.50(15); N(3B)−LiA−N(2A), 103.80(17); C(8A)−N(2A)−C(17A), 120.37(17).

Scheme 2

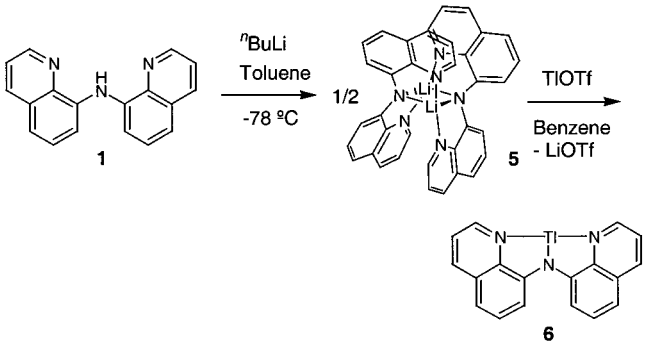

symmetry of which is D_2. The quinoline donor arms of each amido ligand are appreciably canted, and the average angle of intersection defined by their respective mean planes is 58.43°. A simple molecular mechanics minimization of its protonated form, BQAH, predicts an intersection angle of approximately 50°.

While a host of amide complexes of thallium(III) have been reported, stable and well-defined examples of thallium(I) amides are exceedingly rare. The only well-characterized example of which we are aware, $TlN(SiMe_3)_2$, is dimeric in the crystalline state.[23,24] The chelating amido ligand **1** presented a good candidate for supporting a rigorously monomeric thallium(I) amide. Direct exchange of thallium for lithium was effected by addition of TlOTf to a THF solution of **5**. LiOTf precipitated upon benzene extraction of the red residue, and the new red product, [Tl][BQA] (**6**), was isolated and determined to be free of starting material **5** by ^{1}H NMR spectroscopy. An X-ray diffraction study of a single crystal of **6** established that the desired Tl(I) complex of the BQA ligand was indeed the species formed. The X-ray structure of **6** shows a discrete, monomeric complex with a one-to-one adduct between the η^3-BQA ligand

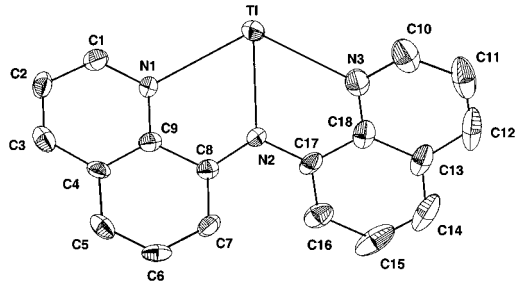

Figure 2. Displacement ellipsoid (50%) representation of [Tl][BQA] (**6**). Selected bond distances (Å) and angles (deg) are as follows: Tl−N(2), 2.397(4); Tl−N(1), 2.689(4); Tl−N(3), 2.802(5); N(2)−Tl−N(1), 63.98(13); N(2)−Tl−N(3), 63.20(15); N(1)−Tl−N(3), 124.98(13); C(8)−N(2)−C(17), 121.6(4); C(9)−N(1)−Tl, 110.8(3); C(18)−N(3)−Tl, 105.7(3); C(1)−N(1)−Tl, 125.0(3); C(8)−N(2)−Tl, 121.0(3); C(17)−N(2)−Tl, 117.1(3).

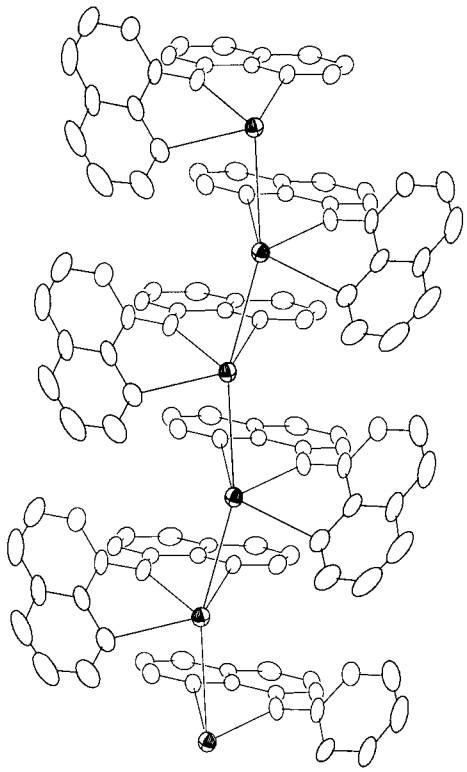

Figure 3. Displacement ellipsoid (50%) representation of [Tl][BQA] (**6**) extended along the crystallographic *a*-axis. The shaded ellipsoids are connected in a zigzag chain highlighting the Tl cations (Tl−Tl1 = 3.5336(5) Å).

and a Tl cation (Figure 2). A possible weak π-stacking or Tl−Tl interaction is observable in the extended structure (Figure 3). Notably, the nearest neighbor Tl cation is located at a distance of 3.5336(5) Å, significantly longer than a generous estimate of the sum of the ionic radii for two Tl(I) cations (ca. 3.28 Å for coordination number of 6).[25] The thallium complexes stack in adjacent columns, each column containing a repeat zigzag arrangement of the monomeric unit. Because of its solubility in benzene, we presume that this zigzag chain structure of **6** in the crystalline state is not present in solution and that **6** is best regarded as a monomeric amido complex of thallium(I).[26]

Important to note is that the BQA ligand, which at first glance might seem to have a small binding pocket, is able to accommodate the very large Tl(I) cation in a well-defined, tridentate fashion. The ligand appears to accommodate this

(23) Klinkhammer, K. W.; Henkel, S. *J. Organomet. Chem.* **1994**, *480*, 167.

(24) This complex was assigned as a monomer in the gas phase. See: Haaland, A.; Shorokhov, D. J.; Volden, H. V.; Klinkhammer, K. W. *Inorg. Chem.* **1999**, *38*, 1118.

(25) Shannon, R. D. *Acta Crystallogr.* **1976**, *A32*, 751.

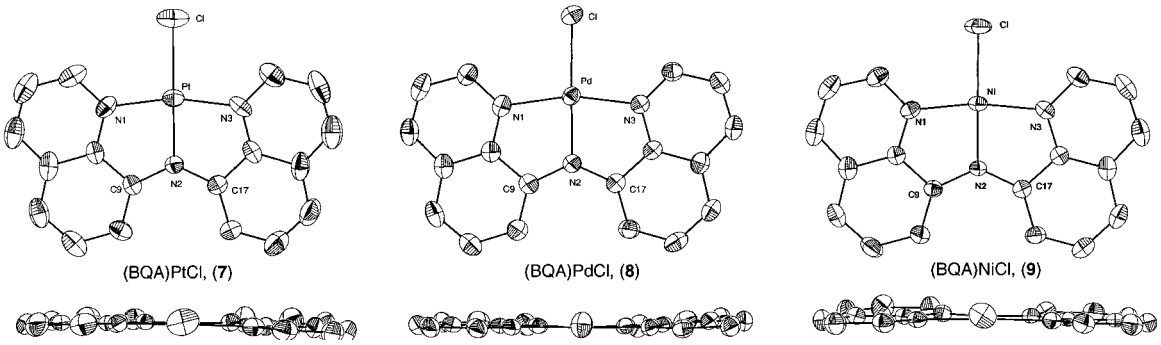

Figure 4. Displacement ellipsoid (50%) representations of the divalent (BQA)MCl complexes **7**−**9** (M = Pt, Pd, and Ni, respectively). Two views are depicted for each structure. The top view is perpendicular to the square plane and the bottom view looks down the Cl−M−N2 axis. Selected bond distances (Å) and angles (deg) are as follows. (BQA)PtCl (**7**): Pt−N(2), 1.966(3); Pt−N(1), 1.994(3); Pt−N(3), 1.999(3); Pt−Cl, 2.3175(11); N(1)−Pt−N(3), 165.34(13); C(17)−N(2)−C(8), 130.9(3); N(2)−Pt−Cl, 177.40(9); N(2)−Pt−N(1), 82.74(12); N(2)−Pt−N(3), 82.70(12); N(1)−Pt−Cl, 97.55(10); N(3)−Pt−Cl, 97.07(10). (BQA)PdCl (**8**): Pd−N(2), 1.962(2); Pd−N(3), 2.0017(19); Pd−N(1), 2.0114(19); Pd−Cl, 2.3298(7); N(2)−Pd−N(3), 82.58(8); N(2)−Pd−N(1), 82.53(8); N(3)−Pd−N(1), 165.10(8); N(2)−Pd−Cl, 178.03(6); N(3)−Pd−Cl, 96.41(6); N(1)−Pd−Cl, 98.45(6); C(17)−N(2)−C(8), 130.4(2); C(17)−N(2)−Pd, 114.81(15); C(8)−N(2)−Pd, 114.53(15); C(18)−N(3)−Pd, 111.71(15). (BQA)NiCl (**9**): Ni−N(2), 1.8586(14); Ni−N(3), 1.8973(16); Ni−N(1), 1.8973(16); Ni−Cl, 2.1779(5); N(2)−Ni−N(3), 84.70(6); N(2)−Ni−N(1), 84.60(6); N(3)−Ni−N(1), 169.10(6); N(2)−Ni−Cl, 174.77(5); N(3)−Ni−Cl, 95.62(5); N(1)−Ni−Cl, 95.23(5); C(1)−N(1)−Ni, 129.25(15); C(8)−N(2)−C(17), 129.05(15); C(8)−N(2)−Ni, 115.49(11); C(17)−N(2)−Ni, 115.43(12); C(10)−N(3)−Ni, 128.84(14); C(18)−N(3)−Ni, 112.42(12).

Scheme 3

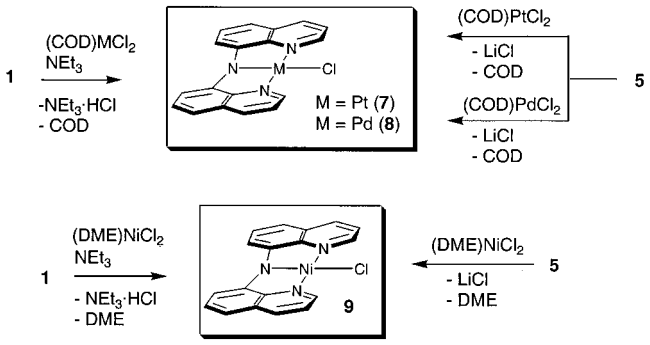

unusually large ion by canting its two quinolinyl arms in such a fashion that the intersection angle of the two planes defined by the quinoline planes is 57.46(11)°. However, this intersection angle is analogous to that found for the lithium dimer **5**. Thus, transmetalation of the small lithium cation for the much larger thallium cation actually effects little conformational change in the ligand morphology. As will be discussed below, this BQA geometry markedly contrasts with that found for the divalent, square-planar complexes of Ni, Pd, and Pt and the previously characterized square-planar copper(II) complex.[11]

III.C. Preparation of Divalent Ni, Pd, and Pt Complexes of BQA Ligand 1. The two methods that proved efficacious for the preparation of divalent monochloride complexes of the group 10 metals supported by BQA were (i) transmetalation with the [Li][BQA] reagent and (ii) dehydrohalogenation using the free acid BQAH in the presence of NEt_3 base. For example, reaction of BQAH/NEt_3 with (COD)$PtCl_2$ in methylene chloride solution generates (BQA)PtCl (**7**) quantitatively with concomitant liberation of cyclooctadiene. Removal of the hydrochloride salt byproduct was accomplished either by ethanol washing of the alcohol insoluble product or by extracting the target complex with benzene and filtering it away from Et_3N·HCl. Alternatively, **7** can be prepared by transmetalation with [Li][BQA] in benzene at 65 °C. Complex **7** is an intensely purple solid that is both air and water stable. The complexes (BQA)PdCl (**8**) and (BQA)-NiCl (**9**) were prepared by similar methods from (COD)$PdCl_2$ and Ni(DME)Cl_2 (DME = dimethoxyethane), respectively. These reactions are summarized in Scheme 3.

III.D. X-ray Structural Study of (BQA)MCl (M = Ni, Pd, Pt). We undertook a comparative X-ray diffraction study of complexes **7**−**9** to determine the adopted BQA ligand geometry for divalent group 10 metal ions.[10] All three complexes crystallized in the space group $P2_1/n$ and, as expected, formed monomeric, square-planar structures. As can be seen in Figure 4, all three complexes are highly planar. Complexes **7** and **8** are virtually isostructural. Notably, the N_3-M-N_1 angle decreases on going from Ni (169.3°) to Pd and Pt (av = 165.2°), reflecting a configurational adjustment when the larger divalent ions are accommodated. This change is not reflected in the $C_8-N_2-C_{17}$ angle about the amido nitrogen donor, which in fact slightly increases (ca. 2°) for Pd and Pt relative to Ni.

III.E. Comparing the Reactivity of (COD)$PtCl_2$ with the Potentially Tridentate Ligands 2-Pyridine-2-yl-ethyl-QAH (2) and *o*-(NMe_2)Ph-QAH (3) and the Bidentate Ligand 3,5-Me_2Ph-QAH (4). Having established that the parent BQA ligand coordinates platinum(II) in a rigorously tridentate fashion, we attempted the preparation of analogous complexes bearing the potentially tridentate ligands **2** and **3**. While reaction of **2** with (COD)$PtCl_2$ afforded an ill-defined product mixture,[27] addition of a stoichiometric amount of **3** to (COD)$PtCl_2$ in the presence of excess triethylamine base effected a rapid color change with concurrent salt precipitation. A ^{1}H NMR spectrum of the isolated crystalline product, however, showed *two* resonances attributable to dimethylamino groups in about a 3:1 ratio; no coalescence was observed on raising the temperature to 80 °C. Resonances originating from a COD-like ligand were also present, establishing that simple displacement of cyclooctadiene had not occurred. Despite successive recrystallizations,

(26) One caveat regarding the preparation of **6** needs to be noted. Although suitable crystals were obtained for the X-ray analysis, ^{1}H, ^{13}C, and ^{19}F NMR spectra of recrystallized samples of **6**, while showing only one BQA-containing species, consistently show trace amounts of THF and triflate anion, which we presume to result from some ill-defined association of LiOTf. Efforts to fully remove these trace impurities, including successive lyophilizations from frozen benzene followed by hydrocarbon extraction and filtration, have thus far been unsuccessful, preventing a successful combustion analysis.

(27) We tentatively assign the primary platinum-containing product of this reaction as {2-pyridin-2-yl-ethyl-QA}Pt(1,2-η^2-6-*σ*-cycloocta-1,4-dienyl), with ligand **2** binding in an η^2-fashion analogous to the well-characterized complexes **10a** and **11** (vide supra). Unfortunately, although LC-MS (ES) corroborates this assignment, its complete isolation and purification has thus far eluded us.

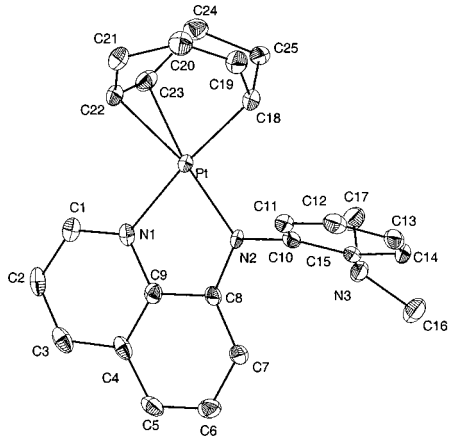

Figure 5. Displacement ellipsoid (50%) representation of (*o*-(NMe_2)-Ph-QA)Pt(1,2-η^2-6-σ-cycloocta-1,4-dienyl) (**10a**). Selected bond distances (Å) and angles (deg) are as follows: Pt−N(2), 2.003(2); Pt−C(18), 2.037(3); Pt−C(22), 2.115(3); Pt−N(1), 2.126(2); Pt−C(23), 2.141(3); C(18)−C(19), 1.489(5); C(18)−C(25), 1.537(5); C(19)−C(20), 1.324(5); C(20)−C(21), 1.484(5); C(21)−C(22), 1.509(5); C(22)−C(23), 1.395(5); C(23)−C(24), 1.523(5); C(24)−C(25), 1.524(5); N(2)−Pt−C(18), 95.93(12); N(2)−Pt−C(22), 156.80(11); C(18)−Pt−C(22), 89.60(13); N(2)−Pt−N(1), 79.45(10); C(18)−Pt−N(1), 171.50(11); C(22)−Pt−N(1), 97.43(11); N(1)−Pt−C(23), 102.22(12).

Scheme 4

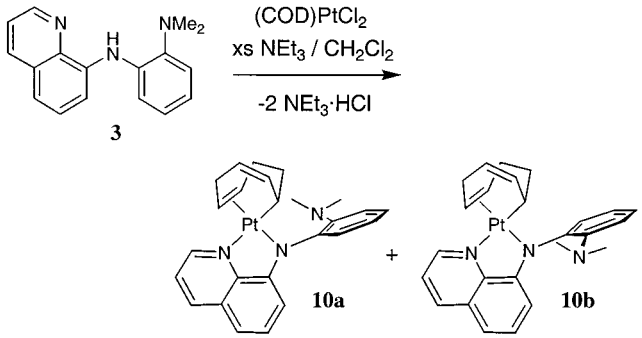

there was no change in the relative intensities of the two dimethylamino resonances implying that the reaction product was likely a mixture of two isomers. On closer inspection of a batch of isolated red crystals, it was determined that two crystalline forms were present; an attempt was made to solve the solid-state structure of each. One of the two crystal types gave a high-quality data set, and its solid-state structure is shown in Figure 5. The reaction product, (*o*-(NMe_2)Ph-QA)Pt(1,2-η^2-6-σ-cycloocta-1,4-dienyl) (**10a**), features ligand **3** as a bidentate rather than tridentate anionic amido ligand, the dimethylamino group being unbound (Scheme 4). The originally neutral cyclooctadiene donor ligand has been transformed to a formally deprotonated anionic ligand that occupies the other two sites of the pseudo-square-planar platinum center. Curiously, the cyclic organic ligand does not bind to the platinum center as a simple η^3 π-allyl ligand. Rather, it binds in an unusual fashion best described as a 1,2-η^2-6-σ-cycloocta-1,4-dienyl ligand. The X-ray structure of **10a** shows the dimethylamino group projecting toward the side opposite the unbound double bond between carbons C19 and C20 of the asymmetric cyclic ring ligand. We infer that a distinct chemical isomer should exist whereby the dimethylamino group projects into the opposite face, and presume this to be the reason two isomers are observed by ^{1}H NMR spectroscopy on a uniform sample of the isolated batch crystals. This isomer is sketched as **10b** in Scheme 4. Hoping to corroborate this assignment with an X-ray diffraction study,

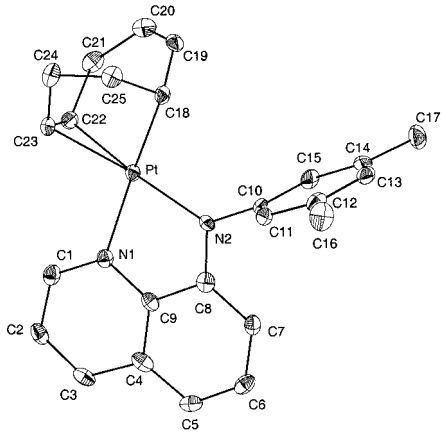

Figure 6. Displacement ellipsoid (50%) representation of (3,5-Me_2Ph-QA)Pt(1,2-η^2-6-σ-cycloocta-1,4-dienyl) (**11**). Selected bond distances (Å) and angles (deg) are as follows: Pt(1)−N(2), 2.008(3); Pt(1)−C(18), 2.048(3); Pt(1)−C(22), 2.123(3); Pt(1)−C(23), 2.124(3); Pt(1)−N(1), 2.135(3); C(18)−C(19), 1.486(5); C(18)−C(25), 1.549(5); C(19)−C(20), 1.324(6); C(20)−C(21), 1.495(5); C(21)−C(22), 1.508(5); C(22)−C(23), 1.395(5); C(23)−C(24), 1.512(5); C(24)−C(25), 1.519(5); N(2)−Pt(1)−C(18), 96.77(12); N(2)−Pt(1)−C(22), 158.63(12); C(18)−Pt(1)−C(22), 89.25(14); N(2)−Pt(1)−C(23), 162.98(13); C(18)−Pt(1)−C(23), 80.62(14); N(2)−Pt(1)−N(1), 79.63(11); C(18)−Pt(1)−N(1), 175.07(13); C(22)−Pt(1)−N(1), 95.31(12); C(23)−Pt(1)−N(1), 101.83(12).

we collected data on the second crystal type of the batch crystals. The data set collected was difficult to solve and was best interpreted as a mixture of two diastereomers in a 3:1 ratio, the major diastereomer being analogous to the structure of **10b**.[28]

Further direct evidence for the simple formulation of **10** as the two spectroscopically distinct isomers **10a** and **10b** was provided by the following data: (i) Combustion analysis of the batch crystals was consistent with the simple empirical formula of complex **10**. (ii) Only one species ($(M + H)^+ = 565$) was observed by LR-MS (electrospray; positive mode) for a batch sample of complex **10** (FW = 564). (iii) The same product was obtained employing (COD)PtI_2 instead of (COD)$PtCl_2$ as the platinum starting material. A space-filling model of **10b** leads us to conclude that facile rotation of the ortho-substituted aryl ring about the N2−C10 axis is not possible, and thus, the two diastereomers become spectroscopically distinct on the NMR time scale. If this interpretation is correct, then preparation of a bidentate ligand variation of **10** without an *o*-dimethylamino group, as is the case for ligand **4**, should lead to a single spectroscopically observable product. Indeed, it was found that when **4** was added to (COD)$PtCl_2$ in the presence of excess triethylamine, a single isomer was observed by ^{1}H NMR spectroscopy at 25 °C and was assigned as the product (3,5-Me_2Ph-QA)Pt(1,2-η^2-6-σ-cycloocta-1,4-dienyl) (**11**). An X-ray structural investigation of the crystallized product (Figure 6) established that **11** has a structure analogous to that of **10a**. In the case of **11**, we presume that facile rotation around the N2−C10 axis is fast on the NMR time scale and equilibrates the methyl positions on the aryl ring that are clearly chemically distinct in the solid-state structure of **11**. Taken collectively, the data establish that ligands **3** and **4** react with (COD)$PtCl_2$ to give similar products, **10** and **11**, with the added complication that complex **10** exists in solution as two observable diastereomeric isomers.

(28) Although disordered, the X-ray data for **10b** show that the geometry around platinum places the amido N-donor trans to the dative bond of the cyclic ring, as is the case for **10a** (see Supporting Information).

Scheme 5

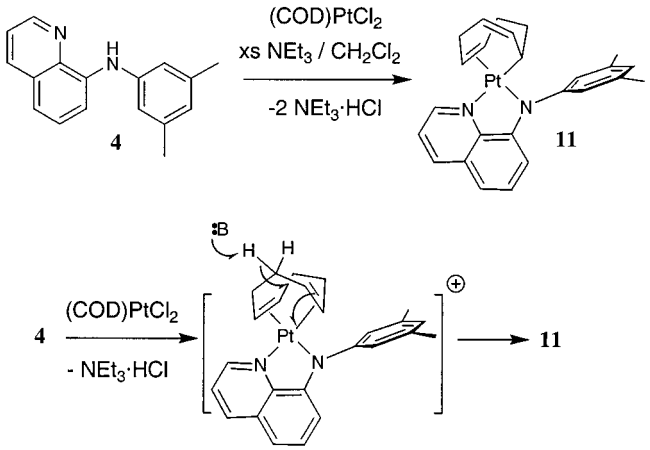

An explanation for the formation of products **10** and **11** remains to be put forward. While we are unaware of similar (1,2-η^2-6-σ-cycloocta-1,4-dienyl) ligands in group 10 chemistry, the literature does provide one precedent for such a ligand. Kubiak and co-workers established that the addition of relatively soft bases to the cationic iridium complex [Ir(triphos)(η^4-1,5-cylcooctadiene)][Cl] effected deprotonation of the cyclic ring and formation of a structurally characterized iridium(I) product, Ir(triphos)(1,2-η^2-6-σ-cycloocta-1,4-dienyl).[29] Scheme 5 postulates a related scenario for the formation of complex **11 (**and by analogy complexes **10a** and **10b**). Ligand **4** coordinates the divalent platinum starting material with concomitant loss of HCl. This results in an unobserved cationic species susceptible to deprotonation by triethylamine base at the C24 position of the cyclic diene ring of **10** (or the related C20 position of **11**). Consistent with this scenario is the following observation: when (COD)$PtCl_2$ reacts with the lithium amide salt of **3**, formed by in situ deprotonation of **3** by ^{n}BuLi, the product yield of **10a,b** is significantly lower and the major byproduct of the reaction is the free acid of ligand **3**. The lithium amide has two competing pathways, one in which it coordinates the platinum center and one in which it acts as the base that deprotonates the cyclic diene ring.

(29) Gull, A. M.; Fanwick, P. E.; Kubiak, C. P. *Organometallics* **1993**, *12*, 2121.

IV. Conclusions

The preparative groundwork for a series of related ligands based upon an 8-quinolinylamine motif has been established. Palladium-catalyzed cross-coupling methods proved very useful for the preparation of **1** and the related amines **2**−**4**, all of which present promising ligands for transition metal chemistry. Establishing the coordination chemistry of these ligands is a necessary first step in their development, and this introductory manuscript illustrates our initial progress into their group 10 chemistry. In contrast to the straightforward tridentate binding of **1** to divalent platinum, we have elucidated a striking difference for ligands **2**−**4**. These ligands react with (COD)$PtCl_2$ to afford unusual examples of coordinated cyclic dienes derived from the COD-containing starting material. We will report on the potential of the systems developed herein for stoichiometric and catalytic transformations in due course.

Acknowledgment. We wish to thank the California Institute of Technology and the Dreyfus Foundation for their generous support of this research through a start-up grant and a Dreyfus Foundation New Faculty Award.

Supporting Information Available: Full details for X-ray structures of compounds **5**−**11**, including tables of positional parameters, displacement parameters, and bond lengths and angles. This material is available free of charge via the Internet at http://pubs.acs.org.

IC010336P